

# SDN-Based Self-Organizing Energy Efficient Downlink/Uplink Scheduling in Heterogeneous Cellular Networks

Seungil MOON<sup>†a)</sup>, Thant Zin OO<sup>†b)</sup>, S. M. Ahsan KAZMI<sup>†c)</sup>, Bang Ju PARK<sup>††d)</sup>, *Nonmembers,*  
and Choong Seon HONG<sup>†e)</sup>, *Member*

**SUMMARY** The increase in network access devices and demand for high quality of service (QoS) by the users have led to insufficient capacity for the network operators. Moreover, the existing control equipment and mechanisms are not flexible and agile enough for the dynamically changing environment of heterogeneous cellular networks (HetNets). This non-agile control plane is hard to scale with ever increasing traffic demand and has become the performance bottleneck. Furthermore, the new HetNet architecture requires tight coordination and cooperation for the densely deployed small cell base stations, particularly for interference mitigation and dynamic frequency reuse and sharing. These issues further complicate the existing control plane and can cause serious inefficiencies in terms of users' quality of experience and network performance. This article presents an SDN control framework for energy efficient downlink/uplink scheduling in HetNets. The framework decouples the control plane from data plane by means of a logically centralized controller with distributed agents implemented in separate entities of the network (users and base stations). The scheduling problem consists of three sub-problems: (i) user association, (ii) power control, (iii) resource allocation and (iv) interference mitigation. Moreover, these sub-problems are coupled and must be solved simultaneously. We formulate the DL/UL scheduling in HetNet as an optimization problem and use the Markov approximation framework to propose a distributed economical algorithm. Then, we divide the algorithm into three sub-routines for (i) user association, (ii) power control, (iii) resource allocation and (iv) interference mitigation. These sub-routines are then implemented on different agents of the SDN framework. We run extensive simulation to validate our proposal and finally, present the performance analysis.

**Key words:** *heterogeneous cellular networks, self-organization, user association, resource allocation, downlink uplink scheduling, Markov approximation*

## 1. Introduction

The heterogeneous cellular networks (HetNets) with macro-cell base stations (MBS) and SBSs increase the complexity in coordination and put constraints on available resources. Another reason is that Software defined networks (SDNs) have evolved with the vision to split the control and data plane and have been very successful among the wired net-

works. This technology can be used to control cells by having a global view of the network, and accordingly, schedule its operation.

Moreover, the existing control equipment and mechanisms are not flexible and agile enough for the dynamically changing environment of HetNet. Management of existing HetNet with this non-agile control plane has become one of the biggest and crucial challenge in order to fulfill users demand. The major challenges of HetNet are (i) user association, (ii) power control, (iii) resource allocation and (iv) interference mitigation problems. Moreover, these sub-problems are coupled and must be solved simultaneously. In this paper, an architectural vision to address the challenges imposed on HetNet. Furthermore, we formulate the DL/UL scheduling in HetNet as an optimization problem and use the Markov approximation framework to propose a distributed economical algorithm.

In HetNet research, there are many works with self-organization algorithm that use game theoretic approaches. In [1], the authors formulated three joint sub-problems of user association, resource allocation and interference mitigation as the maximization of downlink sum-rate with pricing. They proposed a Markov approximation framework to study the convergence in probability. In [2], the authors studied a reinforcement-learning based framework for interference management in small cells networks and proposed self-organizing strategies for interference management in closed-access small cell networks with minimum information required to learn an equilibrium. In [3], the authors employed a semi-Markov decision process to study the admission control problem and design a power control game to reduce energy consumption. The authors in [4] developed a coalition game approach to tackle interference mitigation and reached self-organization solutions that can achieve stable network partitions. The authors in [5] explored up-link scheduling and power allocation problem and used an approximation method to arrive at a sub-optimal solution. However, these works [1]–[5] only consider DL or UL scheduling separately which is real-life must be jointly considered. Moreover, the management and coordination of all the network functions between BSs and UEs is a very challenging issue. Thus, we jointly consider DL/UL scheduling and propose a self-organizing algorithm for the network to dynamically adapt to the changing environment. Next, we employ an SDN controller which decouples the control and data planes to simplify the network manage-

Manuscript received July 22, 2016.

Manuscript revised December 13, 2016.

Manuscript publicized February 18, 2017.

<sup>†</sup>The authors are with the Department of Computer Science and Engineering, Kyung Hee University, Korea.

<sup>††</sup>The author is with the Department of Electronic Engineering, Gacheon University, Korea.

a) E-mail: moons85@khu.ac.kr

b) E-mail: tzoo@khu.ac.kr

c) E-mail: ahsankazmi@khu.ac.kr

d) E-mail: sooyong1320@naver.com

e) E-mail: cshong@khu.ac.kr (Corresponding author)

DOI: 10.1587/transinf.2016NTI0002

ment [6], [7].

The remainder of this paper is organized as follows. Section 2 presents an overview of the system model. We formulate the energy efficient scheduling problem in Sect. 3. Section 4 discusses the Markov approximation framework. In Sect. 5, the SDN Framework for self-organizing energy efficient downlink/uplink scheduling is discussed. In Sect. 6, we present the performance evaluation with numerical and simulation results and we finally conclude this paper in Sect. 7.

## 2. System Model

We consider the downlink and uplink of a HetNet consisting of a fixed set of base stations (BSs) and a randomly located set of user equipments (UEs) denoted by  $\mathcal{B}$  and  $\mathcal{U}$ , respectively as shown in Fig. 1. The network is represented by the graph  $\mathcal{G} = (\mathcal{V}, \mathcal{E})$ , where  $\mathcal{V}$  is the set of nodes (vertices) and  $\mathcal{E}$  is the set of links (edges). The set of nodes in the network consists of the BSs and UEs, i.e.,  $\mathcal{V} = \mathcal{B} \cup \mathcal{U}$ . The set of links contains the downlinks (links from BSs to UEs) and uplinks (links from UEs to BSs), i.e.,  $\mathcal{E} = \mathcal{E}_{DL} \cup \mathcal{E}_{UL}$ . The set of sub-channels (sChs) available to the network is denoted by  $\mathcal{S}$ . There are two types of BSs; the macrocell base station (MBS) and the femtocell base station (FBS), which is also referred to as the small cell base station (SBS). The coverage area of MBS and SBSs will overlapping and each UE is in the range of at least one BS. All BSs are connected to a high speed backhaul with negligible delay. Let  $\psi_i^{DL} \in \Psi$  and  $\psi_i^{UL} \in \Psi$  denote the requested downlink and uplink data rates of UE  $i \in \mathcal{U}$  expressed in bits per second, where  $\Psi$  is the discrete set of QoS levels. Similarly, we also assume that the set per sub-channel transmit power,  $P_{mi}^k$ , (from transmitter  $m$  to receiver  $i$  on sub-channel  $k$ ) is also finite and discrete, i.e.,  $P_{mi}^k \in \mathcal{P} = \{P_1, P_2, \dots, P_{|\mathcal{P}|}\}$ .

### 2.1 Fundamentals

Following the log-distance path loss model, and the positive channel power gain between transmitter  $m$  and receiver  $i$  can be calculated as:  $h_{mi} = 10^{-\mu/10}$ , where  $\mu$  is the total path loss between transmitter  $m$  and receiver  $i$  in decibels (dB). We assume that each receiver  $i$  is capable of measuring  $h_{mi}$  for all transmitter  $m \in \mathcal{V}$ . Let  $\mathcal{V}^k \subseteq \mathcal{V}$  denote the set of transmitters that use sub-channel  $k$ . Then, the interference to the link  $(m, i)$  on sub-channel  $k$  is  $\sum_{n \in \mathcal{V}^k \setminus \{m\}} h_{ni} P_{nj}^k$ . Hence, the instantaneous signal-to-interference-plus-noise-ratio (SINR) for the link  $(m, i)$  on sub-channel  $k$  is:

$$\Gamma_{mi}^k = \frac{h_{mi} P_{mi}^k}{\sum_{n \in \mathcal{V}^k \setminus \{m\}} h_{ni} P_{nj}^k + W N_0}, \quad (1)$$

where  $W$  is the bandwidth of the sub-channel and  $N_0$  is the thermal noise spectral power. Then, the achievable data rate for the link  $(m, i)$  on sub-channel  $k$  is given by

$$R_{mi}^k = W \log_2(1 + \Gamma_{mi}^k). \quad (2)$$

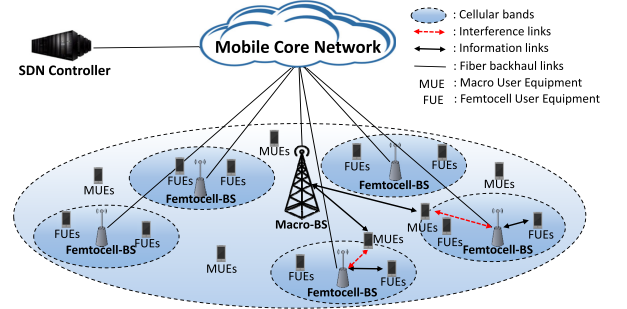


Fig. 1 Network model.

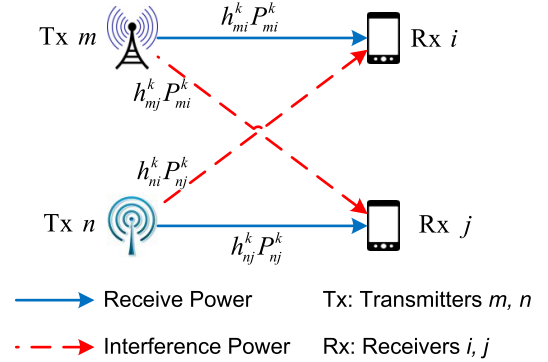


Fig. 2 Receive and interference powers.

Since the available sub-channels for the network is finite and limited, we adopt the dynamic spectrum reuse scheme. We use the concept of *conflict* and *reuse* link pairs (analogous to overlay and underlay spectrum access) to separate the link interference powers into two categories; high interference link pairs which cannot reuse the same sub-channels, or low interference link pairs where spectrum reuse is possible. Consider the two links  $(m, i)$  and  $(n, j)$  as shown in Fig. 2. The sets of *conflict* and *reuse* link pairs are given by:  $\forall k \in \mathcal{S}, \forall (m, i), (n, j) \in \mathcal{E}^k \subseteq \mathcal{E}$

$$\mathcal{E}_{\text{conflict}} = \{(m, i), (n, j) \mid \min\{\Gamma_{mi}^k, \Gamma_{nj}^k\} \leq \widetilde{\Gamma}\}, \quad (3)$$

$$\mathcal{E}_{\text{reuse}} = \{(m, i), (n, j) \mid \min\{\Gamma_{mi}^k, \Gamma_{nj}^k\} > \widetilde{\Gamma}\}, \quad (4)$$

where  $\widetilde{\Gamma}$  is the SINR threshold and  $\min\{\cdot\}$  is the commonly used minimum operator such that  $\min\{a, b\} = a$ , if  $a < b$  and  $\min\{a, b\} = b$ , if  $a > b$ . Note that  $\min\{\cdot\}$  is used since the interfering links may not be symmetric due to disparity in transmit power. In practice, interference measurement and estimation for a link must be made at the receiver side.

## 3. Problem Formulation

### 3.1 Objective

First, the achieved data rates for downlink and uplink between BS  $m$  and UE  $i$  are given by:

$$R_{mi} = \sum_{m \in \mathcal{B}} x_i^m \sum_{k \in \mathcal{S}} y_{mi}^k R_{mi}^k, \quad [\text{DL}] \quad (5)$$

$$R_{im} = \sum_{m \in \mathcal{B}} x_i^m \sum_{k \in \mathcal{S}} y_{im}^k R_{im}^k, \quad [\text{UL}] \quad (6)$$

where  $x_i^m \in \{0, 1\}$  and  $y_{im}^k \in \{0, 1\}$  are the binary decision variables used for user association and sub-channel (resource) allocation, respectively. Similarly, the total amounts of power consumed for respective downlink and uplink between BS  $m$  and UE  $i$  are expressed as:

$$P_{mi} = \sum_{m \in \mathcal{B}} x_i^m \sum_{k \in \mathcal{S}} y_{mi}^k P_{mi}^k, \quad [\text{DL}] \quad (7)$$

$$P_{im} = \sum_{m \in \mathcal{B}} x_i^m \sum_{k \in \mathcal{S}} y_{im}^k P_{im}^k. \quad [\text{UL}] \quad (8)$$

Since our goal is to maximize the energy efficiency of the network, we define the utility function is the ratio of achieved data rate to power consumed, which is expressed in bits per second per watt (bits/s/W). Hence, individual and global utilities are defined as average energy efficiencies given by:

$$u_i(\mathbf{x}, \mathbf{y}, \mathbf{P}) = \frac{R_{mi}}{P_{mi}} + \frac{R_{im}}{P_{im}}, \quad [\text{Individual}] \quad (9)$$

$$U(\mathbf{x}, \mathbf{y}, \mathbf{P}) = \frac{1}{|\mathcal{U}|} \sum_{i \in \mathcal{U}} u_i(\mathbf{x}, \mathbf{y}, \mathbf{P}). \quad [\text{Global}] \quad (10)$$

### 3.2 Constraints

*Unique association:* UE  $i$  can only associate with at most one BS at any time slot, i.e.,

$$\sum_{m \in \mathcal{B}} x_i^m \leq 1, \quad \forall i \in \mathcal{U}. \quad (11)$$

*QoS:* A BS must serve its associated UEs with a minimum QoS requirement, i.e.,

$$R_{mi} \geq \psi_i^{DL}, \quad \forall (m, i) \in \mathcal{B} \times \mathcal{U} \quad [\text{DL}] \quad (12)$$

$$R_{im} \geq \psi_i^{UL}, \quad \forall (m, i) \in \mathcal{B} \times \mathcal{U} \quad [\text{UL}] \quad (13)$$

To satisfy (12) and (13), BS  $m$  must allocate minimum number of sub-channels to UE  $i$ . Assuming that  $R_{mi}^k$  is the same across all sub-channels, we have  $\sum_{k \in \mathcal{S}} y_{mi}^k = \lceil \psi_i^{DL} / R_{mi}^k \rceil$ , where  $\sum_{k \in \mathcal{S}} y_{mi}^k$  represents the total number of allocated sub-channels, and  $\lceil \cdot \rceil$  denotes the ceiling function. Similarly, we have  $\sum_{k \in \mathcal{S}} y_{im}^k = \lceil \psi_i^{UL} / R_{im}^k \rceil$ .

*Interference:* First, the downlinks and uplinks must be allocated orthogonal resources, i.e.,

$$y_{mi}^k + y_{im}^k \leq 1, \quad \forall (m, i) \in \mathcal{B} \times \mathcal{U}. \quad (14)$$

Based on (3) and (4), the interference constraints for conflict and reuse link pairs are given as:  $\forall (m, i), (n, j) \in \mathcal{B} \times \mathcal{U}$

$$y_{mi}^k + y_{nj}^k \leq 1, \quad \{(m, i), (n, j)\} \in \mathcal{E}_{\text{conflict}}, \quad [\text{DL}] \quad (15)$$

$$y_{im}^k + y_{jn}^k \leq 1, \quad \{(m, i), (n, j)\} \in \mathcal{E}_{\text{conflict}}, \quad [\text{UL}] \quad (16)$$

Here, the constraints in (15) and (16) are used to determine whether any link pair can reuse the same sub-channel  $k$  or not. If  $\{(m, i), (n, j)\} \in \mathcal{B}_{\text{conflict}}$ , the spectrum reuse will not be possible. Otherwise, the sub-channel  $k$  can be reused.

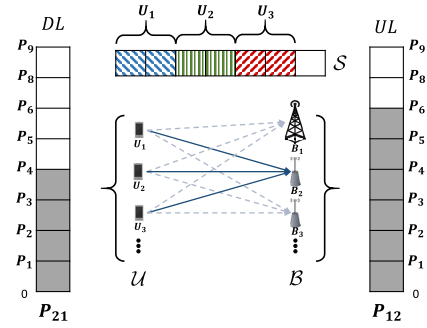


**Fig. 3** The joint optimization problem of DL/UL scheduling: user association, resource allocation, power control.

In other words, we identify the highest interference power links and isolate them by spectrum partitioning.

*Resource:* The available resource to the network must not be exceeded, i.e.,  $\forall (m, i) \in \mathcal{B} \times \mathcal{U}$

$$\sum_{i \in \mathcal{U}} x_i^m \sum_{k \in \mathcal{S}} (y_{mi}^k + y_{im}^k) \leq |\mathcal{S}|, \quad (17)$$

$$\sum_{i \in \mathcal{U}} P_{mi} \leq \widehat{P}_m. \quad (18)$$

Furthermore, the constraint in (17) ensures that the number of sub-channels allocated to UEs by BS  $m$  does not exceed the total number of available sub-channels. Similarly, (18) ensures that the total downlink power of BS  $m$  does not exceed its maximum power  $\widehat{P}_m$ .

### 3.3 Optimization Problem

Our goal is to design a self-organization mechanism that can perform energy efficient scheduling for downlink and uplink under QoS constraints. The scheduling problem contains three sub-problems; (i) user association, (ii) resource allocation, and (iii) power control as shown in Fig. 3. Next, we formulate the joint optimization problem (JOP) as follows:

$$\begin{aligned} \text{JOP : maximize: } & U(\mathbf{x}, \mathbf{y}, \mathbf{P}) \\ & \text{subject to: } (11), (12), (13), (14), \\ & (15), (16), (17), (18). \end{aligned} \quad (19)$$

Due to the unique association constraint given in (11), the number of possible downlinks (UE associations) is reduced from  $2^{|\mathcal{U}| \cdot |\mathcal{B}|+1}$  to  $2 \cdot |\mathcal{B}|^{|\mathcal{U}|}$ . However, the number of possible resource allocations for each downlink is combinatorial, i.e.,  $2^{|\mathcal{S}|}$ . Hence, the solution space of JOP is  $|\mathcal{B}|^{|\mathcal{U}| \cdot |\mathcal{P}|} \cdot 2^{|\mathcal{S}|+|\mathcal{P}|}$ , and no computationally efficient solution for JOP exists. Moreover, JOP belongs to a class of assignment problems which are proven to be combinatorial and NP-hard [8], [9].

## 4. Markov Approximation Framework

The Markov approximation approach can be used to solve JOP because of its ability to solve multiple sub-problems simultaneously without disjoint step-by-step solutions [10],

[11]. First, log-sum-exp approximation is performed, and then, a problem-specific Markov chains is designed to allow distributed implementation.

Let  $f = \{\mathbf{x}, \mathbf{y}, \mathbf{P}\}$  be a network configuration, and  $\mathcal{F}$  be the set of all the feasible configurations that satisfy the constraints in (11), (12), (13), (14), (15), (16), (17), and (18). For ease of presentation,  $U_f = U(\mathbf{x}, \mathbf{y}, \mathbf{P})$ , and JOP be represented by  $\max_{f \in \mathcal{F}} U_f$ . Hence, the equivalent maximum weight independent set (MWIS) problem of JOP is [10]:

$$\max_{f \in \mathcal{F}} U_f \iff \begin{aligned} & \max_{\pi \geq 0} \sum_{f \in \mathcal{F}} \pi_f U_f \\ & \text{s.t. } \sum_{f \in \mathcal{F}} \pi_f = 1 \end{aligned} \quad (20)$$

where  $\pi_f$  is the probability of choosing configuration  $f$ , i.e., its weight, and  $\boldsymbol{\pi}$  denotes the vector of weights  $\pi_f$ . We can view  $\pi_f$  as the fraction of the time that configuration  $f$  is activated.

#### 4.1 Log-Sum-Exp Approximation

The log-sum-exp function,  $g_\beta(U_f)$ , is convex and the closed function [10], [12, p. 93]. Thus, the conjugate of its conjugate  $g_\beta^*(\boldsymbol{\pi})$  is itself, i.e.  $g_\beta(U_f) = g_\beta^{**}(U_f)$  [10], [12, p. 93]. Following the Markov approximation framework, the log-sum-exp approximation of  $\max_{f \in \mathcal{F}} U_f$  yields

$$U_{\max} \approx \frac{1}{\beta} \log \left[ \sum_{f \in \mathcal{F}} \exp(\beta U_f) \right] \triangleq g_\beta(U_f), \quad (21)$$

where  $\beta$  is a positive constant and  $U_{\max} = \max_{f \in \mathcal{F}} U_f$ . Let  $|\mathcal{F}|$  be the size of set  $\mathcal{F}$ , then the approximation accuracy is given by [10], [12, p. 72]:

$$0 \leq |U_{\max} - g_\beta(U_f)| \leq \frac{1}{\beta} \log |\mathcal{F}|. \quad (22)$$

As  $\beta \rightarrow \infty$ , the approximation gap,  $\frac{1}{\beta} \log |\mathcal{F}| \rightarrow 0$ , and thus, the approximation becomes exact.

The log-sum-exp approximation in (21) is equivalent to solving the following optimization problem [10], [12, p. 93],

$$\begin{aligned} & \max_{\boldsymbol{p} \geq 0} \underbrace{\sum_{f \in \mathcal{F}} \pi_f U_f}_{\text{MWIS objective}} - \underbrace{\frac{1}{\beta} \sum_{f \in \mathcal{F}} \pi_f \log \pi_f}_{\text{entropy term}} \\ & \text{s.t. } \sum_{f \in \mathcal{F}} \pi_f = 1. \end{aligned} \quad (23)$$

By finding the Karush-Kuhn-Tucker (KKT) conditions [12, p. 243] of the optimization problem given in (23), we obtain the optimal probability distribution,  $\boldsymbol{p}^*$ , which is given by

$$\pi_f^*(U_f) = \frac{\exp(\beta U_f)}{\sum_{f' \in \mathcal{F}} \exp(\beta U_{f'})}, \quad \forall f \in \mathcal{F}. \quad (24)$$

However, (24) requires *completeness*, i.e. complete information on  $\mathcal{F}$  which can be difficult to find in a practical small cell network due to the large solution space.

#### 4.2 Markov Chain and Transition Rate

The next step is to design a problem specific Markov chain. Each state  $f$  represents a configuration with its corresponding stationary distribution  $\pi_f^*(U_f)$  given by (24) and the set of states  $\mathcal{F}$  contains all possible configurations. As the probability distribution of the Markov chain converges, the configurations will be time-shared according to  $\pi_f^*$ . There exists at least one continuous-time time-reversible ergodic Markov chain whose stationary distribution is  $\pi_f^*(U_f)$  [10].

Let configurations  $f, f' \in \mathcal{F}$  be the states of a time-reversible ergodic Markov chain with stationary distributions  $\pi_f^*(U_f)$ , ( $f \in \mathcal{F}$ ) in (24). Let  $q_{(f \rightarrow f')}$  and  $q_{(f' \rightarrow f)}$  be the non-negative transition rates from  $f \rightarrow f'$  and  $f' \rightarrow f$ , respectively. Then, the two following conditions are sufficient for transition probability design [10]:

- Any two states are reachable from each other,
- (25) is satisfied for all  $f, f' \in \mathcal{F}$ ,

$$\begin{aligned} \pi_f^*(U_f) q_{(f \rightarrow f')} &= \pi_{f'}^*(U_{f'}) q_{(f' \rightarrow f)}, \\ \exp(\beta U_f) q_{(f \rightarrow f')} &= \exp(\beta U_{f'}) q_{(f' \rightarrow f)}. \end{aligned} \quad (25)$$

The balance equation in (25) is significant because complete information on all possible configurations,  $\mathcal{F}$ , is no longer necessary. Furthermore, the Markov chain is time-reversible, and hence, it will converge to  $\boldsymbol{\pi}^*$  with probability one. For our design, we consider the following condition:

$$q_{(f \rightarrow f')} + q_{(f' \rightarrow f)} = \exp(-\tau), \quad (26)$$

where  $\tau$  is a positive constant. From (25) and (26), we have

$$q_{(f \rightarrow f')} = \frac{\exp(-\tau)}{1 + \exp[\beta(U_f - U_{f'})]}, \quad (27)$$

$$q_{(f' \rightarrow f)} = \frac{\exp(-\tau)}{1 + \exp[\beta(U_{f'} - U_f)]}, \quad (28)$$

which are logistic functions of utility differences. Next, we substitute the individual utilities given in (9) instead of global utilities given in (10) for distributed implementation, i.e.,

$$q_{(f \rightarrow f')} = \frac{\exp(-\tau)}{1 + \exp[\beta(u_{i, f_i} - u_{i, f'_i})]}, \quad (29)$$

$$q_{(f' \rightarrow f)} = \frac{\exp(-\tau)}{1 + \exp[\beta(u_{i, f'_i} - u_{i, f_i})]}. \quad (30)$$

Using (29)–(30), we design the Energy Efficient Self-organization Algorithm (EESA) given in Alg. 1. First, EESA builds the conflict and reuse link pairs graph (Line 1–4). The main part of EESA consist of learning (Line 5–8) and consolidation (Line 9–18). When UE  $i$  has a traffic demand, it starts the learning–consolidation process. In learning, each UE randomly chooses a new configuration with exploration probability  $\omega_i$  or stays with previous configuration with probability  $1 - \omega_i$ . The consolidation follows



**Algorithm 1: EESA**


---

**Result:**  $X, Y, P, U$

- 1: **initialization:**  $\mathcal{U}_P := \mathcal{U}, \forall i \in \mathcal{U}_P$
- 2:  $X := \mathbf{0}, Y := \mathbf{0}, P := \mathbf{0}, \Upsilon := \mathbf{0}.$
- 3:  $\tau := 0, \beta_i(0) := 0, \phi_i(t) := 0.$
- 4: Construct (3)–(4) from pilot signals.
- 5: **while**  $t \leq T, \mathcal{U}_P \neq \emptyset, UE i \in \mathcal{U}_P$  **do**
- 6:   **if**  $\phi_i(t-1) = 0$  **then**
- 7:      $x_i(t) := \begin{cases} \text{rand}(X_i) & \text{with prob. } \omega_i. \\ x_i(t-1), & \text{with prob. } 1 - \omega_i. \end{cases}$
- 8:      $P_i(t) := \begin{cases} \min\{P_i^{\max}, P_i(t-1) + \Delta P\}, & \text{with prob. } \omega_i/2. \\ \max\{P_i^{\min}, P_i(t-1) - \Delta P\}, & \text{with prob. } \omega_i/2. \\ P_i(t-1), & \text{with prob. } 1 - \omega_i. \end{cases}$
- 9:   **else**
- 10:     Calculate  $\nu := q(f \rightarrow f')$  using (29)
- 11:      $x_i(t) := \begin{cases} x_i(t-1), & \text{with prob. } \nu. \\ x_i(t-2), & \text{with prob. } 1 - \nu. \end{cases}$
- 12:      $P_i(t) := \begin{cases} P_i(t-1), & \text{with prob. } \nu. \\ P_i(t-2), & \text{with prob. } 1 - \nu. \end{cases}$
- 13:      $\beta_i(n+1) := \beta_i(n) + \beta_{\text{step}}.$
- 14:      $\Upsilon_i(n-1) := \Upsilon_i(n), \forall n \in \{2, \dots, N\}.$
- 15:      $\Upsilon_i(n) := x_i(t).$
- 16:     **if**  $\Upsilon_i(n-1) := \Upsilon_i(n)$  **then**
- 17:        $\omega_i := \max\{0, \omega_i - \omega_{\text{step}}\}.$
- 18:      $\phi_i(t) := 1 - \phi_i(t-1).$
- 19:     Find  $y_{mi}$  in FIFO manner that satisfies (12) and (15).
- 20:     Find  $y_{im}$  in FIFO manner that satisfies (13) and (16).
- 21:     **if** BS  $m$  satisfies (17) **then**
- 22:       Send  $y_{mi} \geq 0$  and  $y_{im} \geq 0$  to UE  $i$ .
- 23:     **else**
- 24:       Send  $y_{mi} := 0$  and  $y_{im} := 0$  to UE  $i$ .
- 25:     Calculate  $u_i(x, y, P)$  using (9).
- 26:     Update  $X, Y, P, U$ .
- 27:     **if**  $\omega_i = 0$  **then**
- 28:        $\mathcal{U}_P := \mathcal{U}_P \setminus \{i\}.$

---

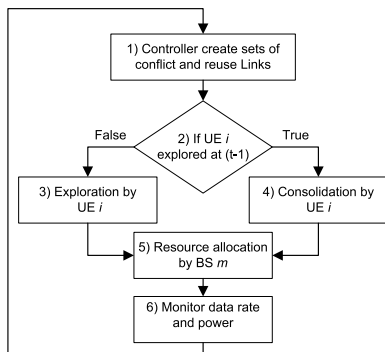


Fig. 4 Block diagram of EESA

each subsequent learning phase where two previous configurations are compared probabilistically. The higher utility configuration is chosen with higher probability. Next, the BSs allocate resource to each link and the matrices are updated (Line 19–26). UE  $i$  repeats this process until  $\omega_i = 0$ . At this point, the UE  $i$  stops the learning–consolidation process and chooses the final configuration for the duration of its request.

### 4.3 EESA

The block diagram of EESA is given in Fig. 4. Learning in EESA consists of two parts, exploration and consolidation, as shown in Fig. 4. In the learning phase, the UE randomly

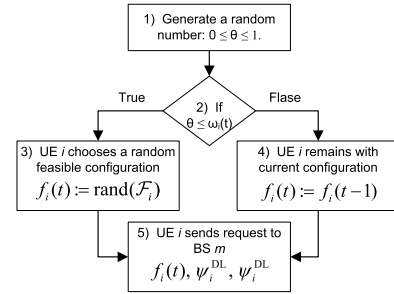


Fig. 5 Block diagram of exploration function

chooses a configuration for experimentation. The configuration including the associated BS, the power level and the allocated sub-channels are stored in history. The achieved data rate and consumed transmit power is also stored in the memory. EESA keeps track of configurations and utilities for two previous time slots. In the consolidation phase, EESA compares the previously stored configurations via the individual utilities stored in history. It then decides probabilistically in choosing a configuration among the stored configurations for the current time slot. Note that higher utility configuration has a higher probability to be chosen. Furthermore, we explain the individual function blocks of EESA in the following paragraphs.

The *exploration* function experiments with new random configurations with an exploration probability. In this case, each UE chooses a configuration randomly with uniform probability distribution. The chosen configuration includes (i) the association control variable,  $x_i^m$ , which randomly chooses a feasible BS with uniform probability distribution (Line 7), and (ii) the power level, which is either increased or decreased by one level with probability 0.5 (Line 8). After every exploration, the exploration probability is decreased until it reaches zero where the UEs no longer participates in exploration of a new configuration.

In *consolidation* function, each UE calculates a transition probability. Then, UEs choose its configurations for time-slot  $t$  from previously observed history at time slot  $(t-2)$  and  $(t-1)$ , probabilistically. A random number  $\phi$  is generated in every consolidation phase through which a configuration among time slot  $(t-2)$  and  $(t-1)$  is chosen. Once the configuration is decided by the UEs, the requests are sent to the respective BSs. Figure 6 presents a block diagram for the consolidation function. Furthermore, the transition probability ensures that the higher utility has a higher probability to be chosen. Thus, after a period of time, configuration chosen at time  $t$  yields better utility than all previous times with a high probability. Due to the properties of the underlying Markov chain, this transition probability ensures that the HetNet converges to a close-to-optimal configuration in probability.

## 5. SDN Framework

Software Defined Network (SDN) framework has two defin-

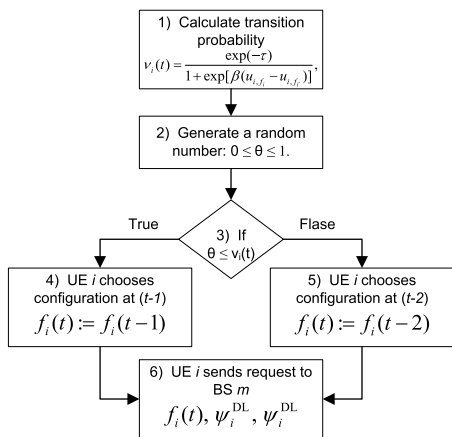


Fig. 6 Block diagram of consolidation function

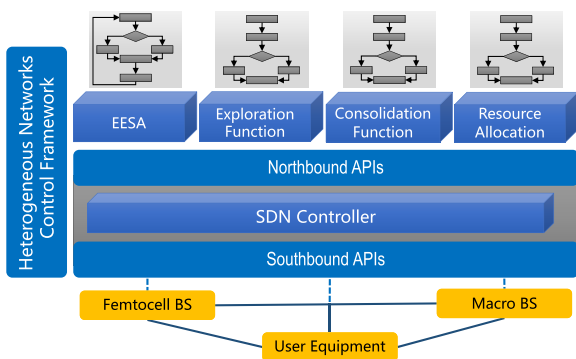
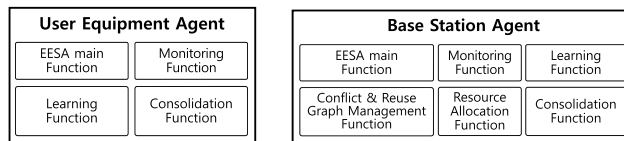


Fig. 7 SDN framework for self-organizing energy efficient DL/UL scheduling

ing characteristics [6]. “First, an SDN separates the control plane (which decides how to handle the traffic) from the data plane (which forwards traffic according to decisions that the control plane makes). Second, an SDN consolidates the control plane, so that a single software control program controls multiple data-plane elements. The SDN control plane exercises direct control over the state in the network’s data-plane elements via a well-defined Application Programming Interface (API).” Algorithm 1 described in Sect. 4 can be implemented distributively as SDN agents in BSs and UEs. However, for ease of management, we employ a SDN controller for logically centralized abstraction and coordination between the BSs and UEs.

5.1 SDN Controller

Figure 7 shows all the components and function of the controller. This architecture abstracts information from each base station and provides a global view to the controller who decides the resources to be allocated. The proposed framework will provide a network resource optimization framework and efficient control mechanism based on SDN for such heterogeneous cellular networks. It provides a self-organizing mechanism that performs energy efficient scheduling for downlink and uplink in the network. Further-



(a) User Equipment Agent (b) Base Station Agent

Fig. 8 Embedded agent in UE and BS

more, the SDN controller is used to achieve higher throughput, reliability and energy efficiency.

5.2 Agent Design Embedded in UEs and BSs

The user equipment and the femtocell base station need some additional components in order to achieve the objective, i.e. throughput maximization of the system subject to interference minimization and power control. This section identifies the agents installed for both the user equipment’s and the femtocell base stations and the controller with the help of sequence diagram.

The user equipment is involved in the tasks of EESA as shown in Fig. 8 (a). The user equipment has the following functions modules

- EESA main function controls individual functions running on the UE Agent.
- Monitoring function monitors the utility and consumed transmit power of the downlink.
- Learning function explores a new configuration with exploration probability  $\omega_i$  or exploits the previous configuration with probability  $1 - \omega_i$ .
- Consolidation function compares two previous configurations and choose higher utility configuration with higher probability.

The base station has the following functions modules as shown in Fig. 8 (b).

- EESA main function controls individual functions running on the BS Agent.
- Monitoring function monitors the utility and consumed transmit power of the downlink.
- Learning function explores a new configuration with exploration probability  $\omega_i$  or exploits the previous configuration with probability  $1 - \omega_i$ .
- Consolidation function compares two previous configurations and choose higher utility configuration with higher probability.
- Conflict and reuse graph management function builds the conflict and reuse link pairs graph.
- Resource allocation function allocates sub-channels to the UE based on the link conflict and reuse graphs.

Now we provide the sequence diagram of EESA. Figure 9 details the process of EESA. EESA algorithm works through the interaction of UE Agent, BS Agent and Controller. It is repeated in order to find the optimal solution. Through the above process, system utility of HetNet is maximized and interference and consumed transmit power are

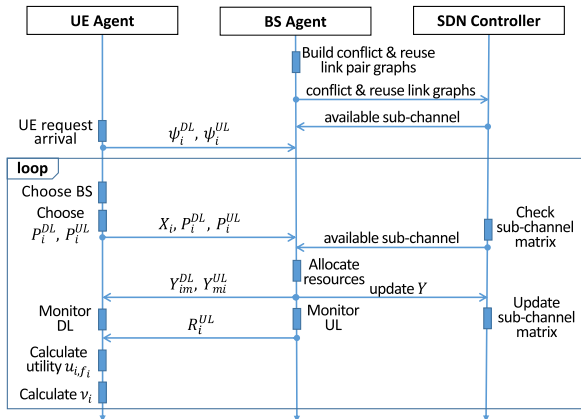


Fig. 9 Sequence diagram of EESA

minimized.

## 6. Performance Evaluation

We perform simulations in MATLAB to evaluate our proposed algorithm. For our experiments, we assume the following: 1) the BSs to be deployed at fixed locations, 2) the UEs are deployed following a homogeneous Poisson Point Process (PPP), 3) user demands (i.e., requested data rate) are discrete and follows a binomial distribution, and 4) SDN controller is collocated with the MBS and the latency between MBS and SDN controller is less than 2 ms. To evaluate our proposed algorithm, we define the normalized performance gap:

$$\varepsilon(t) = 1 - U(t)/U_{\max}, \quad (31)$$

where  $U(t)$  is the utility at time slot  $t$ , and  $U_{\max} = \max_{f \in \mathcal{F}} U_f$ .

We consider a log-distance path loss model for our simulation:  $\mu = \mu_0 + 10 \zeta \log_{10} \frac{d}{d_0} + X_g$ , where  $\mu$  is the total path loss in (dB),  $\mu_0$  is the path loss at reference distance  $d_0$  for the BS,  $d$  is the length of transmission path,  $\zeta$  is the path loss exponent, and  $X_g$  is the attenuation in dB caused by fading. Moreover, we assume that

- for indoors,  $d \leq 20$  m,  $\zeta = 3$ , and  $X_g$  is a Gaussian random variable for shadow fading
- for outdoors,  $d > 20$  m,  $\zeta = 4$ , and  $X_g$  is a Rayleigh random variable for fast fading.

The reference path loss is calculated using two-ray ground reflection model as:

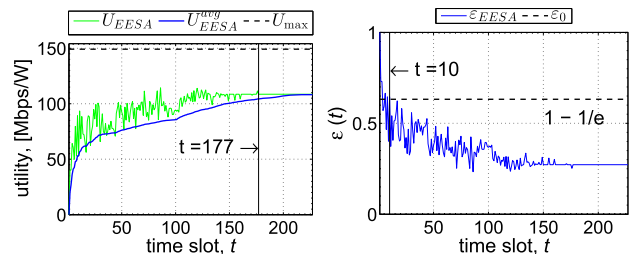
$$\mu_0 = 40 \log_{10}(d_0) - 10 \log_{10}(Gh_t^2 h_r^2), \quad (32)$$

where  $G$  is the transmit antenna gain,  $h_t$  and  $h_r$  are the heights of the antenna of transmitter and receiver, respectively. Simulation parameters are given in Table 1.

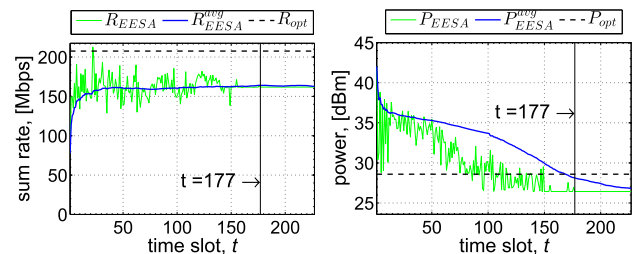
First, we run an experiment to test the convergence of EESA where  $|\mathcal{U}| = 100$  UEs are randomly generated. The results of the experiments are shown in Figs. 10(a)–10(b). Figure 10(a) shows the energy efficiency versus time slot of

Table 1 Default simulation parameters

Quantity	Values
Area of region ( $A$ )	500 m $\times$ 500 m
Static traffic: # of UE ( $ \mathcal{U} $ )	100
UE traffic demand ( $\psi_i^{DL}, \psi_i^{UL}$ )	[0.1, 1] Mbps
# of BS ( $ \mathcal{B}  =  \mathcal{B}_m \cup \mathcal{B}_f $ )	25 = 1 + 24
Total transmit power of BSs	{46, 26} dBm
Antenna gain of BSs ( $G$ )	{12, 6} dBi
Reference distance of BSs ( $d_0$ )	{1000, 20} m
Transmit antenna height of BSs ( $h_t$ )	{30, 3} m
# of sub-channels ( $ \mathcal{S} $ )	12 $\times$ 100
Bandwidth of each sub-channel ( $W$ )	15 kHz
Thermal noise for 1 Hz at 20 °C	-174 dBm



(a) Energy efficiency. (b) Normalized performance gap.

 Fig. 10 Convergence of EESA,  $\omega_{\text{step}} = 0.05$ ,  $|\mathcal{U}| = 100$ .


(a) Achieved sum rate. (b) Total transmit power.

 Fig. 11 Breakdown of utility,  $\omega_{\text{step}} = 0.05$ ,  $|\mathcal{U}| = 100$ .

EESA compared to the optimal energy efficiency  $U_{\max}$ . The normalized performance gap calculated by (31) is shown in Fig. 10(b). Figures 10(a)–10(b) clearly show that EESA converges to a near-optimal solution. During the early time-slots, the magnitude of fluctuations is high since the network has no knowledge and every UE is exploring its possible configurations. As the time goes on, each UE learns about its possible configurations and chooses high utility configurations with high probabilities. Hence, the magnitude of fluctuations becomes smaller and EESA finally converges. This phenomenon is shown in the increasing trend of utility in Fig. 10(a) and the corresponding decreasing trend of the performance gap in Fig. 10(b). Similarly, we can see the corresponding sum rate achieved in Fig. 11(a) and the corresponding total transmit power consumed in Fig. 11(b). Next, we run 100 simulations to test the convergence of EESA and plot the result in Fig. 12. The results show that EESA converges to a near-optimal solution ( $\varepsilon \leq 1 - 1/e$ )

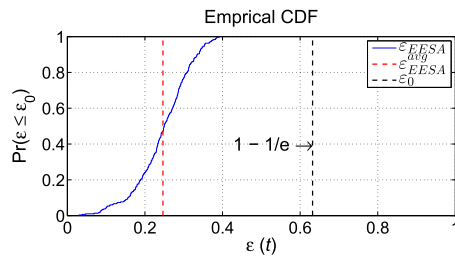


Fig. 12 CDF of  $\varepsilon(t)$ ,  $\omega_{\text{step}} = 0.05$ ,  $|\mathcal{U}| = 100$ .

with probability one. Note that  $1 - 1/e$  is the typical gap for randomized algorithms.

## 7. Conclusions

In this paper, we study about SDN-based self-organizing energy efficient downlink/uplink scheduling in heterogeneous cellular network using the Markov approximation. We consider four joint sub-problems (i) interference mitigation, (ii) user association, (iii) power allocation, and (iv) resource allocation in our problem formulation. Then we apply Markov approximation to solve the formulated problem in Sect. 4. We then propose Energy Efficient Self-Organization Algorithm (EESA) and SDN framework for self-organizing energy efficient downlink/uplink scheduling. Our proposed algorithm is structured into SDN architecture with agents running on MBS, FBSs and UEs. By applying SDN, network information collection and processing become scalable and fast. We then perform simulations to verify our proposal. The simulation results verify that EESA converges to a near-optimal solution.

## Acknowledgments

This research was supported by Basic Science Research Program through National Research Foundation of Korea (NRF) funded by the Ministry of Education (NRF-2014R1A2A2A01005900). Dr. CS Hong is the corresponding author.

## References

- [1] T.Z. Oo, N.H. Tran, W. Saad, J. Son, and C.S. Hong, "Traffic offloading via markov approximation in heterogeneous cellular networks," *IEEE/IFIP Network Operations and Management Symposium*, pp.52–60, April 2016.
- [2] M. Bennis, S.M. Perlaza, P. Blasco, Z. Han, and H.V. Poor, "Self-organization in small cell networks: A reinforcement learning approach," *IEEE Trans. Wireless Commun.*, vol.12, no.7, pp.3202–3212, July 2013.
- [3] L.B. Le, D. Niyato, E. Hossain, D.I. Kim, and D.T. Hoang, "Qos-aware and energy-efficient resource management in ofdma femtocells," *IEEE Trans. Wireless Commun.*, vol.12, no.1, pp.180–194, Jan. 2013.
- [4] Z. Zhang, L. Song, Z. Han, and W. Saad, "Coalitional games with overlapping coalitions for interference management in small cell networks," *IEEE Trans. Wireless Commun.*, vol.13, no.5, pp.2659–2669, May 2014.

- [5] E. Biton, A. Cohen, G. Reina, and O. Gurewitz, "Distributed inter-cell interference mitigation via joint scheduling and power control under noise rise constraints," *IEEE Trans. Wireless Commun.*, vol.13, no.6, pp.3464–3477, June 2014.
- [6] N. Feamster, J. Rexford, and E. Zegura, "The road to sdn: An intellectual history of programmable networks," *SIGCOMM Comput. Commun. Rev.*, vol.44, no.2, pp.87–98, April 2014.
- [7] C.-X. Wang, F. Haider, X. Gao, X.-H. You, Y. Yang, D. Yuan, H.M. Aggoune, H. Haas, S. Fletcher, and E. Hepsaydir, "Cellular architecture and key technologies for 5g wireless communication networks," *IEEE Commun. Mag.*, vol.52, no.2, pp.122–130, 2014.
- [8] D.W. Pentico, "Assignment problems: A golden anniversary survey," *European Journal of Operational Research*, vol.176, no.2, pp.774–793, 2007.
- [9] H. Boostanimehr and V.K. Bhargava, "Unified and distributed QoS-driven cell association algorithms in heterogeneous networks," *IEEE Trans. Wireless Commun.*, vol.14, no.3, pp.1650–1662, March 2015.
- [10] M. Chen, S.C. Liew, Z. Shao, and C. Kai, "Markov approximation for combinatorial network optimization," *IEEE Trans. Inf. Theory*, vol.59, no.10, pp.6301–6327, Oct. 2013.
- [11] S. Zhang, Z. Shao, M. Chen, and L. Jiang, "Optimal distributed P2P streaming under node degree bounds," *IEEE/ACM Trans. Netw.*, vol.22, no.3, pp.717–730, June 2014.
- [12] S. Boyd and L. Vandenberghe, *Convex Optimization*, Cambridge University Press, New York, NY, 2004.



**Seungil Moon** received his B.S. and M.S. degrees from the Department of Computer Science and Engineering at Kyung Hee University, Korea, in 2011 and 2013, respectively. Since September 2013, he is working on his Ph.D. degree in Department of Computer Science and Engineering at Kyung Hee University, Korea. His current research interests include Software-Defined Networking, Network Functions Virtualization, Network Management and Machine Learning.



**Thant Zin Oo** received the B.Eng. degree in electrical systems and electronics at Myanmar Maritime University, Thanlyin, Myanmar in 2008 and the B.S. degree in computing and information system from London Metropolitan University, U.K., in 2008. He received the Ph.D. degree in computer engineering from Kyung Hee University, South Korea in 2017. His research interests include wireless communications, network virtualization, data centers, and sustainable energy.





**S. M. Ahsan Kazmi** received his B.S. degree from University of Engineering & Technology, Lahore. (UET), Pakistan, in the field of Computer Engineering in 2008 and Master's degree in Communication System Engineering from National University of Sciences and Technology (NUST), Pakistan, in 2012. Currently he is pursuing his PhD degree from Kyung Hee University (KHU), South Korea. His research interests includes network optimization for Het-Nets, game theory, and software defined Net-

working for cellular networks.



**Bang Ju Park** received his B.S. (1986), M.S. (1988) degrees in electronic engineering from KyungHee University, Korea and Ph.D. (2006) degree in radio engineering from KyungHee University and Korea Institute of Science and Technology (KIST), Korea. From 1988 to 2012, he worked as a science reporter at JoongAng daily, Korea. From 2008 to 2012, he worked as a visiting professor in the College of Bio-Nano engineering at Gachon University, Korea. In 2013, he moved to Gachon University

where he is now a full professor of the department of electronic engineering and a director of Institute of Bio & Mechatronics. His research interests are electronic devices and radio-manipulation for biomedical instrumental applications.



**Choong Seon Hong** received the B.S. and M.S. degrees in electronic engineering from Kyung Hee University, Seoul, South Korea, in 1983 and 1985, respectively, and the Ph.D. degree from Keio University, Minato, Japan, in 1997. In 1988, he joined Korea Telecom, where he worked on broadband networks as a Member of Technical Staff. In September 1993, he joined Keio University. He worked for the Telecommunications Network Laboratory, Korea Telecom, as a Senior Member of Technical Staff and

the Director of the Networking Research Team until August 1999. Since September 1999, he has been a Professor with the Department of Computer Science and Engineering, Kyung Hee University. His research interests include future Internet, ad hoc networks, network management, and network security. He is a member of ACM, IEICE, IPSJ, KIISE, KICS, KIPS, and OSIA. He has served as the General Chair, a TPC Chair/Member, or an Organizing Committee Member for international conferences such as NOMS, IM, APNOMS, E2EMON, CCNC, ADSN, ICPP, DIM, WISA, BcN, TINA, SAINT, and ICOIN. In addition, he is currently an Associate Editor of the IEEE Transactions on Network and Service Management, International Journal of Network Management, and Journal of Communications and Networks and an Associate Technical Editor of the IEEE Communications Magazine.